Chapter 6

ELECTRICAL PROSPECTING METHODS IN VOLCANIC AND GEOTHERMAL ENVIRONMENTS

G.V. KELLER and A. RAPOLLA
Department of Geophysics, Colorado School of Mines, Golden, Colo. (U.S.A.)
Institute of Geology and Geophysics, University of Naples, Naples (Italy)

INTRODUCTION

Electrical prospecting methods, both galvanic and inductive, have proved to be among the most useful geophysical methods in volcanology. The physical parameter that is determined by these methods is the rock resistivity or conductivity, which is strongly temperature-dependent, and, obviously, the knowledge of the horizontal and vertical variation of temperature is of the most concern in the study of active volcanic environments.

This last term is used here in its widest sense to include all the areas in which geothermal manifestations occur. Moreover, the study of the physical and structural characteristics of the lower crust and of the upper mantle below an active volcanic area is not considered separately from the study of the most superficial part of the crust — where volcanism actually takes place. Electrical methods may, in this respect, give useful information either from shallow or deep investigations. In this article, we will discuss the electrical properties of volcanic rocks, mainly with respect to their resistivity—temperature relationship, considering first the high temperature range, and then the normal temperature range when the presence of water in the rock pores becomes the main weight.

Examples of the application of some electrical prospecting techniques, taken mostly from the authors' experience, are reported. The article ends with a sketch of the proper exploration programme in an active geothermal area and a few examples of the possibility of making use of precursive electrical and magnetic anomalies for prediction of volcanic eruptions.

ELECTRICAL PROPERTIES OF VOLCANIC ROCKS

The electrical properties of volcanic rocks in active volcanic environments can be discussed in much the same way as those of rocks in general (Keller, 1971a), with the exception that the effect of temperature on such electrical properties is of more concern than is usually the case.

Volcanic rocks and igneous rocks in general, are the result of the solidification of a silicate melt. Silicate rock-forming minerals are unique from the viewpoint of their electrical properties, in that they are solid electrolytes. Electrical conduction in these compounds takes place by ionic processes in ionic-bonded crystals. Generally, the force exerted on ions in an ionic-bonded crystal structure by an applied electric field is smaller than the ionic-binding forces. However, electrolytic conduction does take place in such compounds because of inherent lattice and thermally induced imperfections. The former kind of imperfections, which are responsible for the low-temperature (up to 700°C) conductivity, consist of weakly bonded impurities, or defects in the crystal. The latter, which are responsible for the high-temperature conductivity, consist of the displacement of ions from the lattice by thermal vibrations. Two main trends have, in fact, been observed in experimental works on the relation between temperature and conductivity carried out on volcanic and igneous rocks: a low-temperature trend, which is a function of the structure of the specific sample and of its thermal history, and a high-temperature trend, which seems to be an intrinsic property of a material, varying little from sample to sample.

In both cases, there is a relationship between the logarithm of the conductivity and the inverse absolute temperature, and the overall relation may be expressed as a sum of several terms, by the equation:

$$\sigma = A_1 e^{-U_1/kT} + A_2 e^{-U_2/kT} \tag{1}$$

where the indices 1 and 2 refer to the low-temperature and high-temperature portion of the relation, respectively; the parameters A_1 and A_2 depend on the number of ions available for conduction, and on their mobility; U_1 and U_2 are the activation energies; k is Boltzmann's constant; T is the absolute temperature. Values of the above parameters are given in Table I (Keller and Frischknecht, 1966).

As can be seen from Table I, A_2 is many orders of magnitude higher than A_1, which explains the very rapid conductivity increase as thermally induced crystal imperfections predominate over inherent crystal imperfections.

TABLE I

Values of A_1, A_2, U_1 and U_2

Rock	A_1 (mho/cm)	A_2 (mho/cm)	U_1 (eV)	U_2 (eV)
Granite	$5 \cdot 10^{-4}$	10^5	0.62	2.5
Gabbro	$7 \cdot 10^{-3}$	10^5	0.70	2.2
Basalt	$7 \cdot 10^{-3}$	10^5	0.57	2.0
Peridotite	$4 \cdot 10^{-2}$	10^5	0.81	2.3
Andesite	$6 \cdot 10^{-3}$	10^5	0.70	1.6

A review of the experimental work on the temperature-induced variation of conductivity on volcanic and igneous rocks was made by Parkhomenko (1967). Following the results of researches quoted by this author, resistivity-temperature curves for acidic and intermediate rocks, such as andesite, diorite, granite, etc., show several discontinuities, each one representing a change in the electrical conduction processes. Experimental results for basic and ultrabasic rocks are practically the same, only curves for such rocks seem to be more regular. The discontinuities observed from 800 to 1000°C and around 1200°C should be related to the melting process of different mineral phases.

It is interesting, however, to note that the first discontinuity was generally found at relatively low temperatures, about 500—700°C. We recall here that as a result of experimental studies on the temperature variation of the viscosity of lava samples, Imbò (1968) noticed that there was a low-temperature discontinuity on the cooling curve, around 600°C, varying from sample to sample, depending on their petrographic nature. According to the above author, this discontinuity is a result of a sudden increase in viscosity from about 10^8 to 10^{16} poise. Such a fact may also

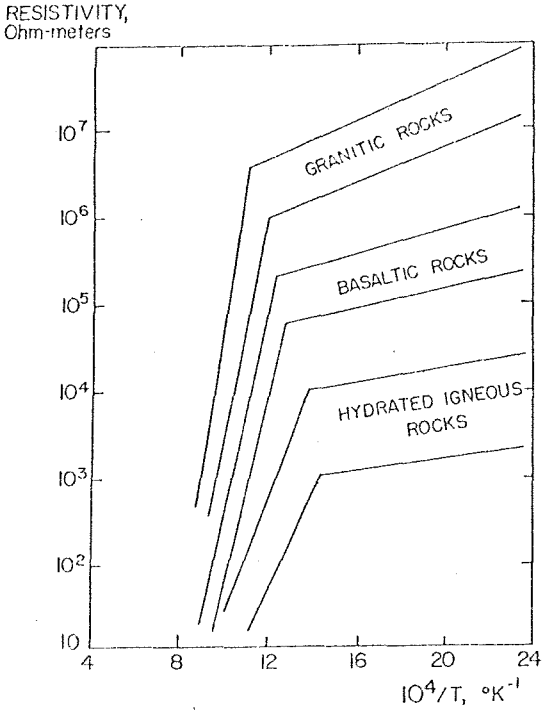

Fig.1. Generalized summary of values reported for the resistivity of dried rocks as a function of temperature (from Jacobson, 1969).

explain the low temperature discontinuity, as observed in the resistivity-temperature curves.

Fig.1 (Jacobson, 1969) gives a generalized summary of the resistivity of dry rocks as a function of temperature. Volcanic and igneous rocks differ from other rocks with respect to their electrical properties, as well as in another respect, i.e., for these rocks resistivity is frequency-dependent. Fig.2 shows the variation of resistivity of a granodiorite sample as a function of frequency at various temperatures (Keller and Frischknecht, 1966). The frequency-dependence of solid electrolytes, such as the granodiorite-forming minerals, also depends on the temperature. At low temperatures there is an inverse resistivity-frequency relationship, while at high temperatures the resistivity is nearly constant.

Direct measurements of conductivity of molten rocks as they naturally occur in volcanoes are very scarce. Frischknecht (1967) reports a measurement of electrical resistivity of molten basalt in the lava lake of the Kilauea-Iki crater, Hawaii, obtained by a two-loop frequency-domain electromagnetic technique. A value of 2.5 Ωm was obtained, which is about 40 times lower than the resistivity of a sample of the same rock

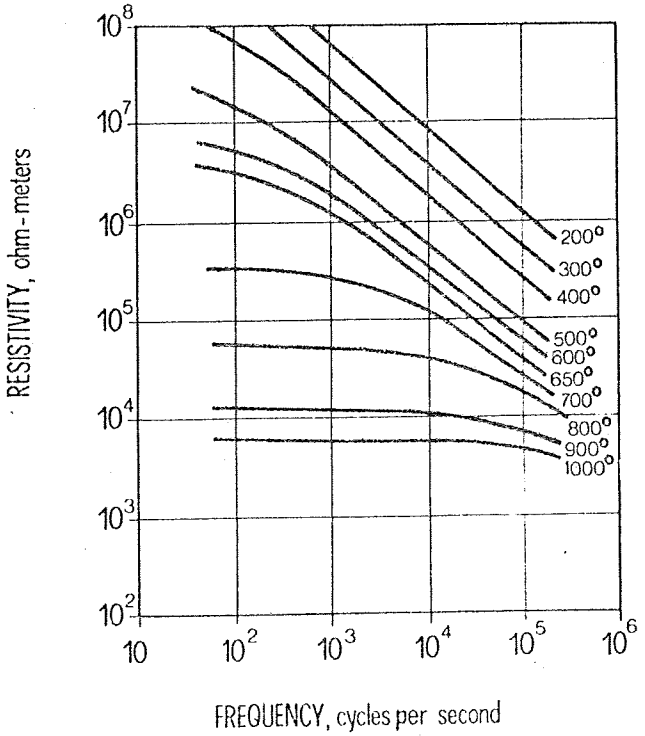

Fig.2. Resistivity of a granodiorite sample measured as a function of frequency at various temperature (from Keller and Frischknecht, 1966).

immediately below the melting point, and many hundreds of times lower than the resistivity of a basaltic lava flow as normally found at the surface of the volcano.

Finally, the presence of even a very small amount of water in a silicate rock may change the temperature-induced variation of conductivity of a rock. Experimental works made by Watanabe (1970) on basaltic samples show that the trends of proportionality between conductivity and temperature are different for samples with traces of water from those obtained with dry samples, in that the presence of water markedly increases the electrical conductivity. Results of the above study led Watanabe to confirm the hypothesis that differences in electrical conductivity in the lower crust and the upper mantle deduced by geomagnetic and magneto-telluric depth soundings may be interpreted as due to differences in water content.

At normal temperature, so long as a porous rock contains even a small amount of water in its pore space, the electrical properties of the rock will be dependent almost entirely on the electrical properties of that water and the manner in which the water is distributed through the rock. Many laboratory studies carried out on water-bearing porous rocks have indicated that the relationship between resistivity and water content in a rock may be represented by the empirical equation:

$$\rho = a\rho_{\mathrm{w}}\, \phi^{-m} \tag{2}$$

where ρ is the bulk resistivity of the rock, ρ_{w} is the resistivity of the water contained in the rock, ϕ is the porosity of the rock expressed as a volume fraction, and a and m are experimentally determined parameters required to make the equation fit a specific group of data. Most of the measurements reported in the literature have been made on clastic detrital rocks, in as much as such information is used primarily in the evaluation of oil reservoir rocks. Relatively few measurements have been made on igneous rocks or volcanic rocks.

Fig.3 is a plot of measured values of resistivity as a function of porosity for a suite of basalt samples from Hawaii (Keller et al., 1972a). The resistivities are plotted in terms of the dimensionless ratio, ρ/ρ_{w}, which is a quantity known as the formation resistivity factor (F), providing the pore structure is filled with electrolyte. The porosity is taken to be equal to the water content of the samples. While the plotted points do exhibit a trend toward higher resistivity for lower water contents, as is indicated by the dashed trend line on Fig.3, the scatter of the points is pronounced. This scatter from the trend line is considered to be a consequence of the small size of the rock samples used for the measurements and the large size of the pore structures in the basalt. With larger samples, it might be expected that the geometry of the pore structures in a single sample would come closer to a more reasonable average than was the case for the small samples used.

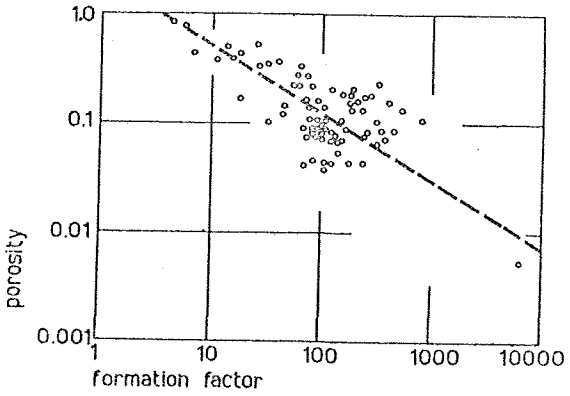

Fig.3. Scatter plot of resistivities and porosities measured on small samples of Hawaiian basalts.

To some extent, this idea is substantiated by result of resistivity measurements made on samples of rhyolitic volcanic rock from the Oak Springs Formation (Miocene?), from southern Nevada, in Fig.4 (Keller, 1960). Here many measurements were made on small samples, but only the average resistivities for groups of samples with similar porosities are plotted. It may be seen that the averages fall close to a trend line characterized by the equation:

$$\rho = 4.5\ \rho_w\ \phi^{-1.7} \tag{3}$$

Carrara and Rapolla (1972) report measurements of resistivity of loose pyroclastics of medium to high porosity and of potassic alkalitrachytic nature from the Phlegraean Fields volcanic area, Italy. Resistivity values of the water solution saturating the above rocks are also given. The relation between rock resistivity and water resistivity which was obtained is expressed in this case by the equation:

$$\rho = 2.8\ \rho_w\ \phi^{-1.7} \tag{4}$$

The multiplying factors, 4.5 and 2.8, in both eq.3 and 4 are considerably larger than the values normally observed for sedimentary or crystalline rocks (Parkhomenko, 1967). This means that for a given water content a volcanic rock will be several times more resistive than a sedimentary rock. Fig.5 shows the trend lines that have been reported for both igneous and sedimentary rocks for comparison with the trend-line found law. This behaviour may be easily rationalized by considering that much of the porosity in volcanic rocks is in the form of bubbles, which are connected by fine pore structures. Most of the resistance to current flow is met in the fine connecting pores, so that the large volume of porosity in

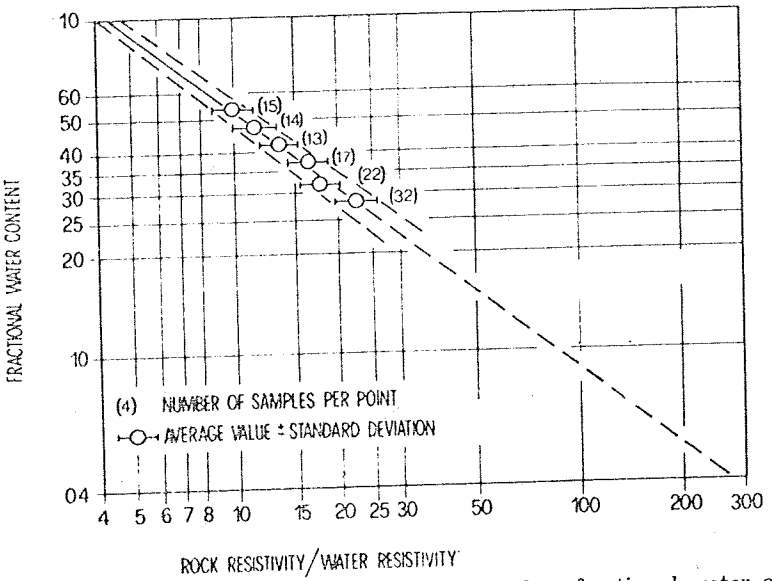

Fig.4. Cross plot between porosity (expressed as fractional water content, W) and formation factor ($F = \rho/\rho_W$) for small samples of water-saturated rhyolitic tuff from southern Nevada.

the bubble-like structures does not contribute much in determining the overall resistivity of the rock.

Empirical relationships, such as those shown in Fig.5, are useful in predicting the resistivity of a volcanic rock, if the porosity and the conductivity of the water are known. The conductivity of the water contained in rocks arises as a consequence of the presence of ions in solution. Conductivity, then, depends on the concentration of ions, or the salinity, and on factors which modify the mobility of ions, such as temperature.

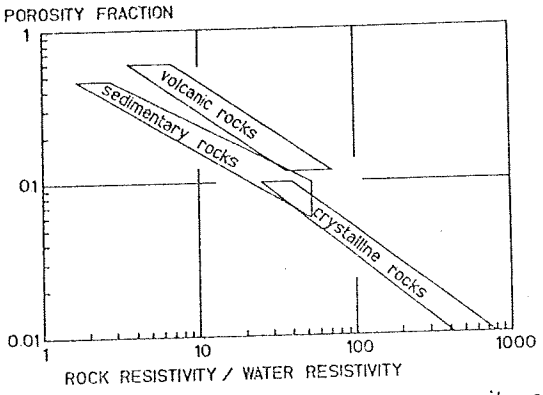

Fig.5. General relationship between porosity and formation factor for rocks with various types of porosity.

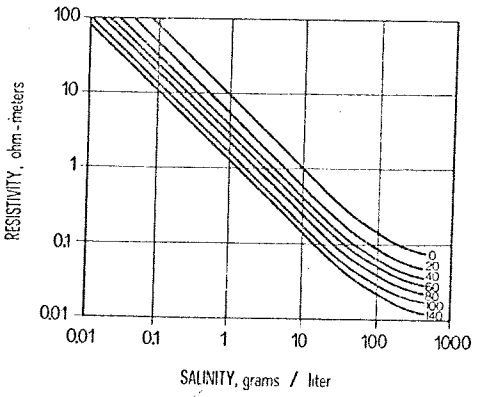

Fig.6. Resistivity of sodium chloride solutions as a function of concentration and temperature (from Keller and Frischknecht, 1966).

At normal temperatures, the relationship between electrolyte conductivity and ion concentration is well known. Curves for this relationship for sodium chloride solutions are shown in Fig.6, for temperatures up to 100°C, the boiling temperature of water at a pressure of 1 atm. There is not a great deal of difference between the conductivities for various salts, and in all cases the rate of change with temperature is about 2% per degree Centigrade.

In geothermal areas, the temperature in the ground may be much higher than 100°C, but, under these conditions, the relationship between conductivity of an electrolyte and temperature is less well known. At temperatures up to 374.4°C, water has a well-defined boiling point, which increases with increasing pressure. At temperatures above this, no clear distinction can be made between the liquid state and the gaseous state. In either case, if water has a density close to unity, one may expect it to act as an electrolyte, while if the water has a density significantly less than unity, it may not act as an electrolyte. This is indicated on the pressure—volume curves in Fig.7, where the pressures and temperatures at which an aqueous solution has no higher conductivity than at 20°C are shown as a heavy dashed line (Eisenberg and Kaufmann, 1969). To the right of this dashed line, water quickly becomes non-conductive (steam), while, to the left of this line, it may be said that temperature has rendered the water anomalously conductive.

The variation of electrolyte resistivity with temperature in dilute solutions of various common salts has also been studied by Quist and Marshall (1966, 1968). The curves shown in Fig.8 based on their published results indicate how much the resistivity of a dilute solution of sodium chloride, such as might represent a ground water in a volcanic rock, can be lowered from its value at 20° C, by raising the temperature. The two curves shown

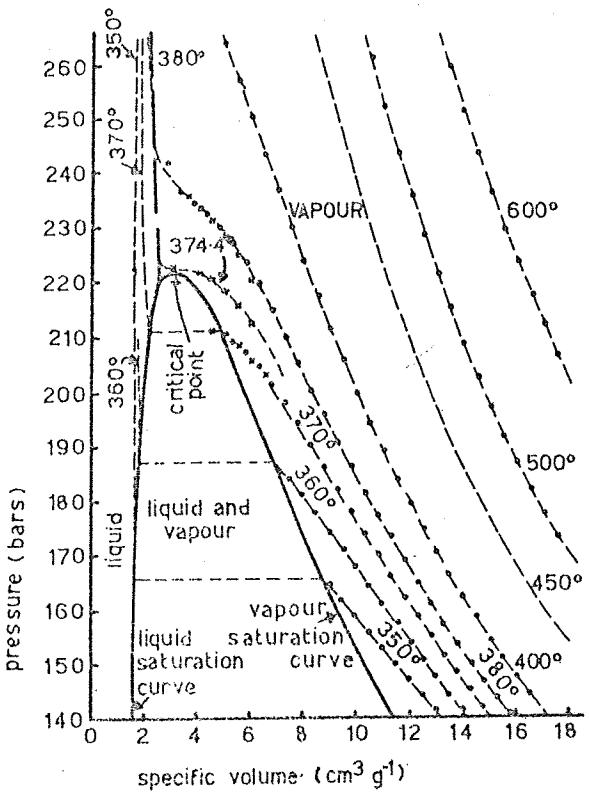

Fig.7. Pressure—volume relationship for H_2O near the critical point (from Eisenberg and Kaufmann, 1969). It is to be expected that an aqueous electrolyte will become a poor conductor at specific volumes above 2.0, as indicated by the dashed line.

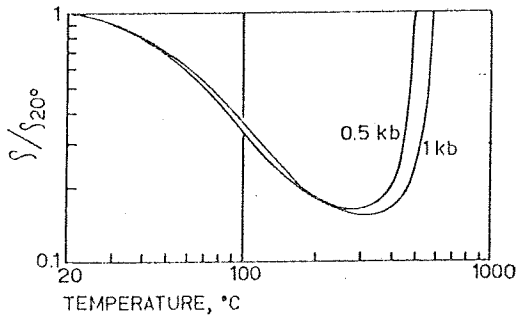

Fig.8. Variation of the resistivity of a dilute solution of sodium chloride with temperature at pressures of 0.5 and 1.0 kbars.

apply for pressures of 0.5 and 1.0 kbar, as indicated. In volcanic rocks with a density of 2.0, pressure increases at a rate of 1 kbar/5,000 m of burial; the pressures of concern in a geothermal system should lie in the range from 0.2 to 1.0 kbar. At these pressures, the resistivity of water passes through a minimum value, at a temperature of 280—300°C, with the minimum being less than the resistivity at 20°C by a factor of approximately 7. Because the resistivity of a water-saturated rock varies in the same manner as the resistivity of the water itself, we can argue that the resistivity of volcanic rocks in a geothermal area may be reduced by a factor of about 7 by the effects of temperature.

Continental volcanic rocks are commonly saturated with water having a relatively low salt content. In such cases, it is important to recognize that the value for ρ_w, the resistivity of the water in the pore structures of a rock, may be different from the value for ρ_w determined from samples of water produced from the rock. This difference arises because the pore water interacts in a variety of ways with the solid minerals forming a rock. One important interaction is the hydrolysis of clay minerals in which ions held in exchange positions on the clay minerals, go into solution in the pore water and increase the total salinity. These ions cannot be stripped from the clay minerals completely, and so, when water is removed from a rock, these ions remain behind. The amount of salinity added by ion exchange depends on the quantity of exchange ions available (the amount of clay present, in general), and on the amount of water present. Cation exchange capacities are normally given as a certain number of milli-equiv. of exchange ions per 100 g of clay minerals, with typical values ranging from about 10 for an inert clay, like kaolinite, to 100 or more for active clays, such as montmorillonite (Keller and Frischknecht, 1966). As an example, if a volcanic rock were to contain 0.1 g of active clay per cm^3 of rock, the amount of exchange ions added to the pore water would be about 100 micro-equiv. For sodium ions, considering that they are placed in solution in pore water comprising one-third the volume of a rock, the added salinity would be approximately 6,900 p.p.m. Clay contents in fresh volcanic rocks are normally much smaller than the 5% assumed in this example, but it is clear that for volcanic rocks saturated with fresh or brackish water, the contribution to conductivity from exchange ions must be considered.

Very few determinations of the effective salinity of water in place in the pore structure have been reported for volcanic rocks. One set of such determinations has been reported by Keller (1962) for measurements made on samples of rhyolitic tuff, from the Oak Springs Formation (Miocene?), southern Nevada. The pore-water resistivity was determined by measuring the resistivity of the samples twice, first when they were resaturated with distilled water in the laboratory, and second when they were resaturated with a brine having a high known salinity. In the first

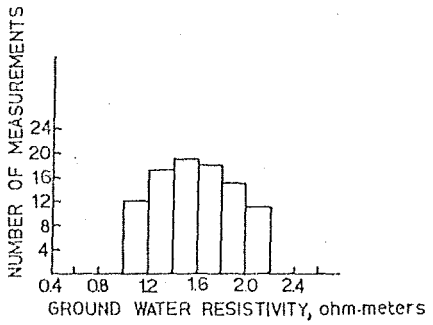

Fig.9. Apparent pore water resistivities determined on samples of rhyolitic tuff from southern Nevada.

case, the water introduced into the pore structure would have a salinity comprised of the salt left behind in the rock and the ion exchange salinity. In the second case, because the salinity of the solution forced into the pore structure was high, the effect of the ions added by exchange processes could be neglected. With this assumption, the resistivity of the original pore water can be computed with the formula:

$$\rho_{w_1} = \rho_{w_2} \frac{\rho_1}{\rho_2} \left(\frac{S_1}{S_2} \right)^n \tag{5}$$

where ρ_{w_1} and ρ_{w_2} are the resistivities of the original water and a solution with 50,000 p.p.m. NaCl, respectively, ρ_1 and ρ_2 are the rock resistivities for the sample saturated with water having the resistivity ρ_{w_1} or ρ_{w_2}, respectively, and S_1 and S_2 are the fractions of pore spaces filled with water in the natural and resaturated states, respectively. A value of 2 was arbitrarily selected for the parameter n. Since the ratio of saturations, S_1/S_2, was almost unity, errors in the choice of n had very little effect on the accuracy of the values for water resistivity, ρ_{w_1}. A histogram showing the distribution of values found for ρ_{w_1} is given in Fig.9. The range in values was found to be from 1.04 to 2.13 Ωm, with an average of 1.6 Ωm. Water produced from springs near where the samples were taken had a resistivity of approximately 40 Ωm. The difference is caused by the addition of exchangeable ions to the pore water.

In addition to having electrical properties which depend on pore structure in microscopic detail, volcanic rocks can be considered to have electrical properties as a consequence of their megascopic structures. Volcanic rocks are layered rocks, to a first approximation. Keller (1968) reviews various methods for describing the average electrical properties as a sequence of layered rocks, in which the individual layers may have different resistivities. In fact, the macroscopic bedding can be considered as resulting in a gross electrical anisotropy of the rock, because current will flow more easily along the direction of lamination of the rock than across

it. The average resistivity for current flow normal to the planes of layering may be defined as:

$$\rho_{tr} = \frac{1}{H} \int_0^H \rho(z)\, dz \tag{6}$$

where $\rho(z)$ is the actual resistivity of the rock as a function of the coordinate normal to the layering, z, and H is the total thickness of the layered sequence over which the average is taken. Similarly, the average conductivity for current flow parallel to the planes of layering may be defined as:

$$\sigma_l = \frac{1}{H} \int_0^H \sigma(z)\, dz \tag{7}$$

where $\sigma(z)$ is the actual conductivity of the rock as a function of the coordinate normal to the layering.

The resistivity, ρ_{tr}, will not be the reciprocal of the conductivity, σ_l, unless all the layers in the section have the same actual resistivity. In general, they do not, and the sequence appears to be anisotropic in electrical properties. A coefficient of anisotropy may be defined as:

$$\lambda = \sqrt{\rho_{tr}\, \sigma_l} \tag{8}$$

In order to determine the macroscopic average electrical properties and the coefficient of anisotropy, it is necessary to have detailed measurements of the actual resistivity through the section, such as are provided by electrical well logs. An electric log obtained from a well drilled in the basalts of the Columbia River Plateau (Rattlesnake Hills Unit No. 1, Benton County, Washington, U.S.A.) is shown in Fig.10. As may be seen, the actual resistivity varies over wide ranges as a function of depth. D.B. Jackson (personal communication, 1972) has computed the average resistivities and coefficients of anisotropies for three depth intervals and

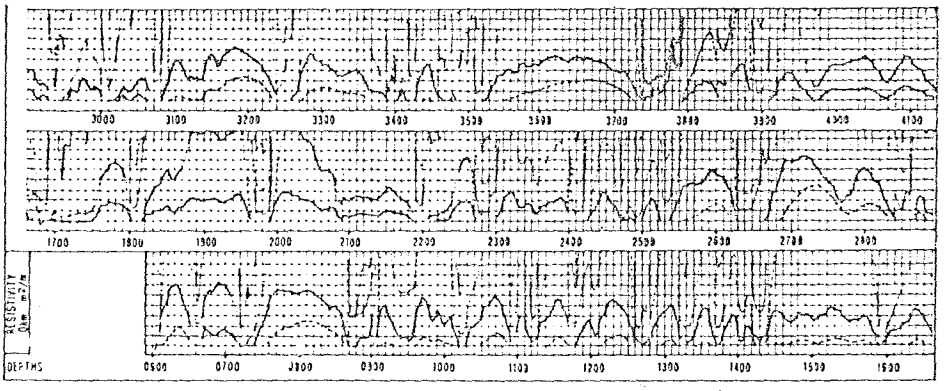

Fig.10. Electrical resistivity log of Rattlesnake Hills Unit No. 1, Benton County, Washington.

TABLE II

Average resistivities determined from an electric log of the Rattlesnake Hills Unit No. 1, Benton County, Washington, U.S.A.

Depth interval (ft.)	Average longitudinal conductivity (mho/m)	Average transverse resistivity (Ωm)	Coefficient of anisotropy
600— 4,100	0.00485	893	2.08
4,100— 6,900	0.0174	150	1.61
6,900—10,600	0.00617	634	1.98

obtained the results listed in Table II. These values for the coefficient of anisotropy are relatively large when compared with values for sedimentary-bedded rocks (Keller, 1968).

Similar results have been reported for determination of anisotropy made from electric logs of the Portage Lake series of volcanic rocks of Precambrian age from the Lake Superior region, U.S.A. (Keller, 1961).

ELECTRICAL SURVEYING METHODS IN ACTIVE VOLCANIC GEOTHERMAL AREAS

The considerations of the factors which determine the electrical properties of a volcanic rock, described in the preceding section, allow us to construct a picture of the exploration problems involved in locating a geothermal system in volcanic rocks. A geothermal system might develop as shown in Fig.11: intrusion of a magmatic body at the base of a sequence of porous rocks, probably volcanic in nature, may provide the

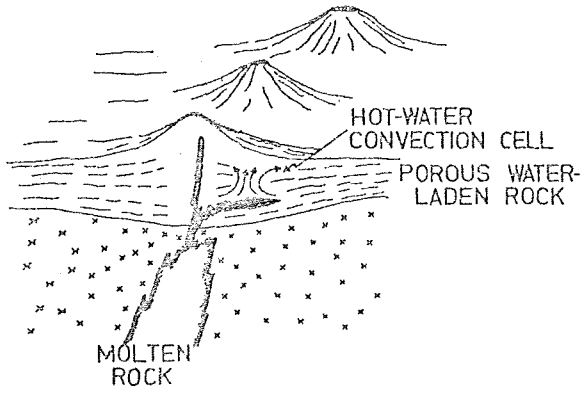

Fig.11. Idealized model of tectonic conditions that can cause the development of a hydrothermal circulation system.

heat source to drive the geothermal system. The water heated at the base of the porous section will expand and rise towards the surface, causing a convection cell to develop. The hot water may discharge at the surface, in the form of hot springs and fumaroles, or if the water table is well below the surface, the hot water may spread out laterally, with no great thermal activity apparent at the surface. Development of geothermal systems like this depends on the existence of an appropriate vertical permeability in the porous section following intrusion of the magmatic body. If the permeability is too great, the convection cell will develop rapidly, and the water in the cell will be heated only slightly. If the permeability is too low, the temperature may rise well above the boiling point for the water in the rock, and a hydrothermal explosion will take place. If the permeability is just right, the water in the convection cell will rise just fast enough that it is heated to a temperature near its boiling point, either slightly above or slightly below. In this case, the geothermal system will have temperatures in excess of 200° C, and the electrical resistivity will be reduced to the minimum possible value, as indicated from Fig.8.

If this is a realistic model of a geothermal system, it comprises an immense target for electrical prospecting techniques. The cell will have an area of ten square kilometers or more, if it is large enough to be of commercial interest, and a vertical extent of several kilometers. The resistivity in the cell should be lower than the resistivity in the surrounding rock by a factor of about 7. It would be difficult to miss a target of this size with any of the conventional electrical prospecting methods, and so the choice of one method or another will depend largely on the operational ease with which a survey can be conducted.

Because many geothermal systems occur in volcanic rocks, the surface characteristics will make some types of electrical survey preferable to others. In volcanic terrains, the surface may be quite rugged and have high resistivity, so that methods based on the use of moving electrode contacts are at a disavantage relative to methods which use inductive coupling or fixed electrode sources. At present, it appears that the most effective electrical surveying techniques for geothermal exploration are dipole mapping (Furgerson, 1970), electromagnetic sounding (Keller, 1971b) and magneto-telluric sounding. Examples of the use of these methods and one regarding the more conventional direct current (DC) sounding method will be given in the following paragraphs.

Dipole mapping

In a dipole mapping survey, as the expression is used here (Furgerson, 1970), a large amount of electric current is caused to flow in the earth between two electrode contacts, situated within a few kilometers of the target area. As the current flows through the ground from this "dipole"

source, its flow pattern will be governed in detail by variations in resistivity in the ground, to a depth comparable to the offset distance at which measurements are made. Inasmuch as the dipole source is fixed in location, while many measurements of electric field are made about it, any electrical non-uniformities near the source will affect all the measurements similarly, and the variations in the characteristics of the electric field from observation point to observation point will be indicative of the electrical structure of the ground, primarily in the vicinity of the measuring points. Having the source fixed in location for many measurements greatly simplifies the patterns of apparent resistivity which appear in the data, in comparison with the data obtained with the conventional moving-source profiling techniques.

The general scheme of a dipole mapping survey is indicated in Fig.12. Normally, the source dipole length is in the range from 1 to 10 km. Because it is necessary to use several tens of ampères of current in order to provide measurable electric fields at a distance of 5—10 km from the source, it is necessary to have low-resistance ground contacts at the ends of the source dipole. In volcanic areas with a high resistivity at the surface, such electrode contacts may be obtained by drilling holes several tens of

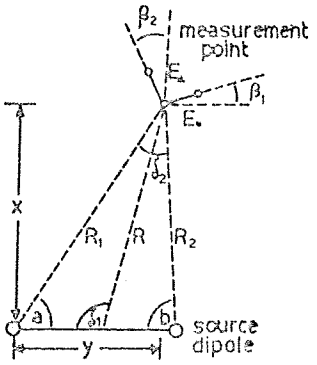

PARALLEL $\rho_{\parallel} = \dfrac{2\pi}{(\cos a/R_1^2)+(\cos b/R_2^2)} \dfrac{E_{\parallel}}{I}$

PERPENDICULAR $\rho_{\perp} = \dfrac{2\pi}{\sin a/R_1^2 - \sin b/R_2^2} \dfrac{E_{\perp}}{I}$

TOTAL-FIELD $\rho_a = \dfrac{2\pi R_1^2}{[1+(R_1/R_2)^4-2(R_1/R_2)^2\cos\delta_2]^{1/2}} \dfrac{E_\tau}{I}$

CONDUCTANCE $s_a = \dfrac{[1+(R_1/R_2)^2-2(R_1/R_2)\cos\delta_2]^{1/2}}{2\pi R_1^2} \dfrac{I}{E_\tau}$

Fig.12. Layout of electrodes for a dipole mapping survey and formulas used in computing apparent resistivity.

meters deep, and by placing lengths of pipe in the holes for electrodes. In some areas, metal road culverts may also serve as good grounds.

A prime power source with a capacity of from 10 to 50 kVA is required for dipole mapping surveys. This power is used to form a step wave in the ground, with periods of reversal ranging from 5 to 50 sec. Long periods are required, so that there are no problems with skin-depth limitations in the highly conductive volcanic rocks through which the current must flow. Usually, an asymmetrical wave form is used, so that it is possible to assign a polarity to the voltage detected at the receiving sites.

The current field from a source dipole is mapped by measuring voltages between electrode pairs at many points about the source dipole. In as much as the direction of current flow at a measurement site is quite unpredictable, the total voltage drop must be determined by making measurements with two electrode pairs oriented at right angles to one another and adding these voltages vectorially. The electric field is then assumed to be the ratio of voltage drop to the separation between the measuring electrodes. Measurements are made with receiving electrode separations of usually 10—100 m.

Electric fields are measured at distances from the source dipole usually ranging up to 5 or 10 km. Measurements are also made close to the dipole, but the principal advantage in using the dipole mapping technique lies in the ability to make measurements at distances of several kilometers from the source. At these distances, the current penetrates to considerable depths, and the resultant electric field measurements characterize the properties of the rocks about the measurement sites to depths typically of the order of several kilometers.

The electric-field data acquired in a dipole mapping survey may be converted to apparent resistivity values using several different formulae (see Fig.12). A "parallel-field apparent resistivity" may be computed by using only the component of electric field intensity measured in the direction parallel to the source dipole. A "perpendicular-field apparent resistivity" may be computed by using only the component of electric field intensity measured in the direction perpendicular to the source dipole. A "total-field apparent resistivity" may be computed by using the magnitude of the electric field intensity, assuming that the direction of the total field is the same as it should be in an uniform earth.

It should be recalled that an apparent resistivity is the actual resistivity of the earth only if the earth is completely uniform. When the earth is not uniform, each of the apparent resistivity values described above can be affected in a different way, and so each of them is useful in studying different types of earth structures. Experience has shown that the most meaningful apparent resistivity value for surveys in geothermal areas is the total-field apparent resistivity, because these values come closer to the actual resistivity at the measurement site when there are pronounced

lateral changes in resistivity. The parallel-field and perpendicular-field apparent resistivities are useful in accentuating variations in an area where the actual resistivity is relatively uniform. In an area of complex electrical structure, these values fluctuate widely, and may even be negative.

If resistant basement is present at depths less than the distance from the measurement sites to the source dipole, the apparent resistivity computed from the total electric field will increase linearly with the distance. As a consequence, a contour map of apparent resistivities will exhibit a pattern of elliptical resistivity contours at distances greater than the depth to basement. In this case, it is more convenient to compute an apparent value of conductance, S_a, from the total electric field, using the lowermost formula on Fig.12. The conductance of a sequence of rocks is defined as:

$$S = \int_0^H \sigma\,(z)\,\mathrm{d}z \tag{9}$$

(Note that this is the same as eq.7, the definition of longitudinal conductivity, except that the expression is not divided by H, the thickness of the section.)

An example of a conductance map based on dipole mapping surveys is shown in Fig.13. The area shown is the volcanic province from North Island, New Zealand, extending from the National Park Volcanoes in the

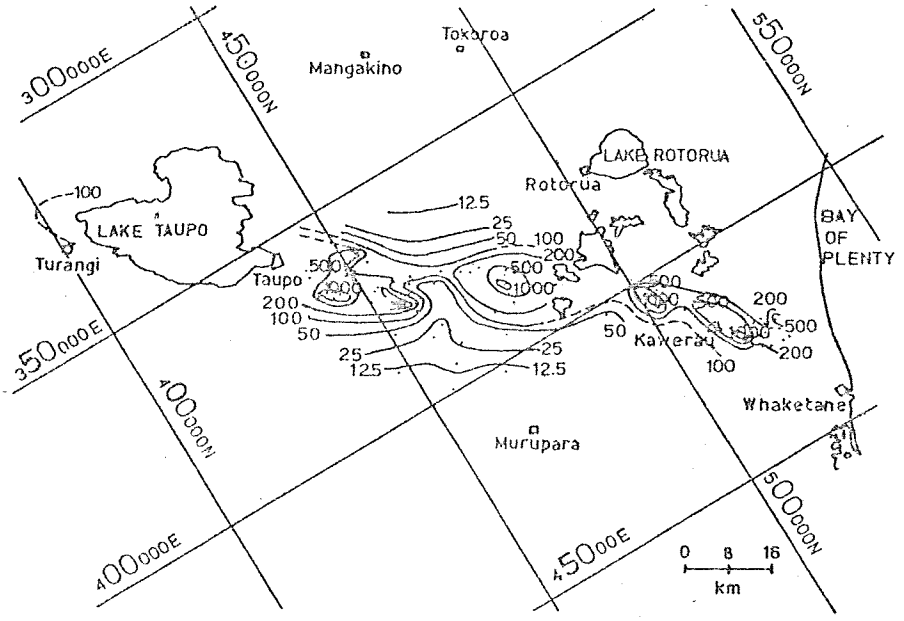

Fig.13. Conductances mapped in a dipole survey of the volcanic regions of North Island, New Zealand.

south to the Bay of Plenty in the north. The measurements contoured were not all made from a single dipole source, but rather from 16 dipole sources located among the trend of the volcanoes. Dipole sources ranged in length from several kilometers to ten kilometers. Current strengths were 30—60 A. The well-known thermal areas are indicated by high values of conductance, reaching 1,000—2,000 mho at Wairaki, Broadlands, Waiotapu and Kawerau. The conductance is only 10—15 mho in areas on either side of the thermal belt.

DC sounding

DC sounding methods for measuring the variation with depth of the earth resistivity have been widely used in geothermal volcanic environments. Making use of a DC sounding, a curve of apparent resistivity vs. spacing is obtained. Several methods are widely used which differ in the way the electrode contacts are arranged on the earth surface.

Three main groups may be considered: one in which the voltage difference between two electrodes is measured; another one in which the voltage gradient is determined by two very closely-spaced electrodes; and finally one in which the curvature of the potential field is measured. Examples of the three arrangements are the Wenner symmetrical quadripolar array, the Schlumberger asymmetrical quadripolar array, and the dipole-dipole array, respectively. In spite of the simplicity of these methods and of the high grade of accuracy which may presently be obtained both in the field measurements and in the interpretation techniques, several problems arise in the use of this method in active volcanic environments.

Lateral variations of resistivity which are commonly found in these areas may lead to a completely erroneous interpretation. Moreover, if a high-resistivity layer is present at the surface, the direct current will penetrate such a layer only with great difficulty, in addition to the fact that its presence may cause serious problems for obtaining a sufficiently good earth contact. Finally, DC sounding methods are best used in looking for resistive targets, as the greater the resistivity of the ground, the higher the amplitude of the signal to be measured. Therefore, when a low resistivity layer is present at depth, as happens in active geothermal fields, the signal to be measured becomes lower and lower in amplitude, and difficult to determine exactly. From a series of soundings, isoresistivity maps relative to one or more horizons at depth, which are of interest, may be eventually obtained, providing very useful data on the vertical and horizontal extension of the geothermal system.

Carrara and Rapolla (1972) report data from several shallow Schlumberger DC soundings carried out in the Phlegraean Fields volcanic

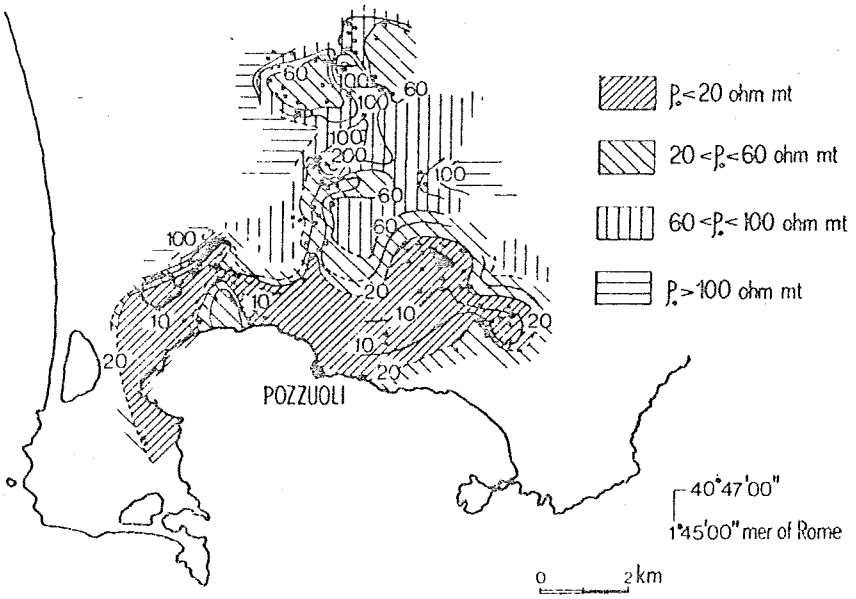

Fig.14. Isoresistivity map of the water-saturated layer. Phlegraean Fields, Italy.

area, Italy, in order to delimite horizontally the local geothermal system. system.

Soundings were deepened, so that they reached the water-saturated (phreatic) layer, whose topographic level was already known. This knowledge made a fairly precise deduction of the phreatic layer resistivity possible as the ambiguity in the interpretation arising from the interconnection between depth and resistivity was in such a way almost overcome. It was thus possible to obtain a meaningful isoresistivity map relative to the phreatic horizon (Fig.14). Lateral variation of resistivity was then ascribed to salinity and temperature variation, where a lithological homogeneity of the host rock could be assumed. An area of low resistivity (less than 20 Ωm) was thus delimited; this should correspond to the most active geothermal area in the Phlegraean Fields. An average salinity content of 1.2—2.6 g/l NaCl equivalent, and an average temperature higher than 32°C for the water solution, was then inferred for this area.

Electromagnetic sounding

In the dipole mapping and DC sounding methods, the surface material in the area being mapped must be conductive enough to permit the measuring electrodes to make contact. In some volcanic areas, the surface may be covered with ash or recent flows, with such a high resistivity that a

contact cannot be obtained. In these cases, it is necessary to use an electromagnetic induction method, which does not require electrode contacts. Both loop-source and grounded-wire source electromagnetic methods have been used in geothermal exploration (Keller, 1971b). Generation of an electromagnetic field by passing a time-varying current through a grounded wire is preferable to the use of an ungrounded loop as a source because of the problems involved in laying out a large-source loop. However, a grounded-wire source requires that there is some location within 5 or 10 km of the suspected geothermal target where the source dipole can be grounded adequately.

Jackson and Keller (1972) describe the application of a time-domain electromagnetic sounding technique, developed at the Colorado School of Mines (Harthill, 1969; Jacobson, 1969; Silva, 1969), to exploration for geothermal activity around Kilauea Volcano in Hawaii. They used a system which closely resembles the dipole mapping setup shown in Fig.12. An electromagnetic field was generated by passing a step-wave of current through a grounded length of wire. The electromagnetic field at a receiver site was detected by using a multiturn loop of wire laid on the ground, rather than with electrode pairs. The geometric relationship of the source to the target area is shown in Fig.15. In this survey, a source cable 2.8 km long was used, grounded in soil on the flanks of Mauna Loa Volcano, away from the area where recent flows from Kilauea Volcano make grounding difficult. The primary power source was a 15-kVA motor-generator set, with the output voltage stepped up from 220 VAC to 660

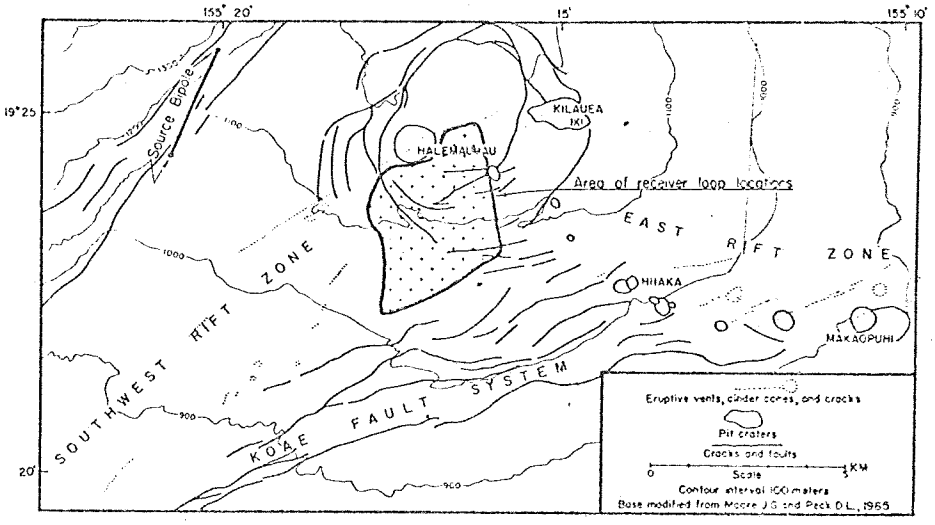

Fig.15. Map of the summit of Kilauea Volcano, Hawaii, showing the locations of the dipole source and induction receivers used in the electromagnetic survey.

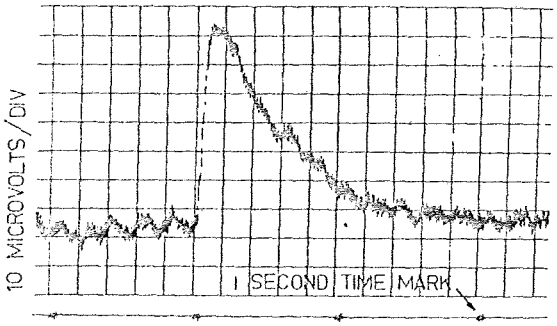

Fig.16. Example of transient electromagnetic coupling recorded during the electromagnetic survey of the summit of Kilauea Volcano, Hawaii.

VAC with a transformer before being rectified and switched to provide current steps in the source cable. The intervals at which current flow in the source wire was reversed were sufficiently long (15 sec) that each reversal could be considered as a current step of infinite duration. As the time required for current to reverse direction on switching was about 10 msec, the reversal of current could be considered as a step-like change.

The induction coil receiver, used to measure the vertical component of magnetic induction, consisted of a 304-m length of 26-conductor cable, laid on the ground in the form of a square, and connected so that the 26 conductors were in series and formed a continuous loop. The voltage generated in this loop was filtered to attenuate frequencies above 10 Hz, then recorded on an oscillograph; the record shown in Fig.16 is typical.

The manner in which such recorded transients are processed to obtain resistivity sounding curves is discussed in detail by Jackson and Keller (1972). Actually, the procedure consists in computing an apparent resistivity from the data from the formula:

$$\rho_a = \frac{2\pi R^4 \, V(t)}{3 \, AM \sin \beta} \tag{10}$$

where M is the moment of the source (the product of current and wire length), A is the area of the receiving loop, β is the angle between the grounded wire source and the radius vector to the centre of the loop, R is the distance between the centre of the wire source and the centre of the loop receiver, and $V(t)$ is the measured voltage at a specific time, t. In time-domain sounding, it is considered that the later parts of the transient coupling are affected by resistivity structures at greater depths than the early parts. Therefore, time can be roughly associated with depth of penetration. A plot of apparent resistivity vs. time, as shown in Fig.17, is analogous to a curve of apparent resistivity vs. spacing, as obtained in conventional DC sounding. An interpretation may then be made of the apparent resistivity plot by comparing it graphically with families of

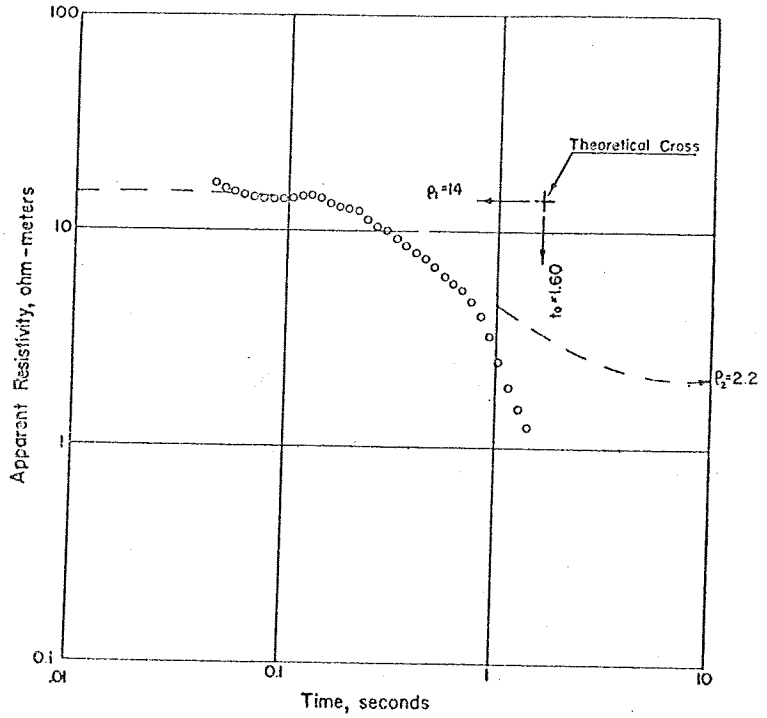

Fig.17. Conversion of a transient coupling curve to an apparent resistivity vs. time curve.

theoretical curves, computed for various combinations of layers. Such curves are available for wire-to-loop soundings for two layers (Silva, 1969) and three layers (King, 1971). The soundings made about the summit of Kilauea Volcano appeared to represent an earth structure made up of two layers; an upper layer with a resistivity of 8—24 Ωm, and a lower zone, with a resistivity of 1—2 Ωm. It must be recognized in this interpretation that an electromagnetic method is largely insensitive to the presence of highly-resistive superficial rocks. Several DC soundings were made in the same area, by using a standard Schlumberger sounding technique (Fig.18), and these indicated a near-surface layer a few tens of meters thick, with a resistivity of 1,000—10,000 Ωm. A few of the electromagnetic soundings indicated that the first 100 m from the surface may have a high resistivity. The first layer mapped with the electromagnetic soundings is most probably basalt with moderate amounts of fresh water in the pore space, migrating downward to the water table or making up the water table. The second layer, the top of which varies approximately between one kilometre below sea level to 200 m above sea level (see Fig.19; note that

the average elevation of the survey area is about 1,100 m above sea level), has a resistivity of about 2 Ωm.

Detailed deformation studies of the summit area (Kinoshita et al., 1974) show that deformation centres associated with the activity of Kilauea Volcano lie mostly within the region defined by the contours on top of the 2-Ωm resistivity layer, which suggests a direct relation between the low resistivity layer and summit deformation. Moreover, numerous small earthquakes have their hypocentres in the vicinity of the 2-Ωm mound (Koyanagi and Endo, 1971).

All of these lines of evidence suggest that the magma reservoir feeding the summit activity of Kilauea Volcano lies beneath the 2-Ωm mound. The contrast in resistivity between the material in this mound and the surrounding rock of the upper layer seen with the electromagnetic soundings is appropriate for the contrast that would result from heating in a geothermal system (see Fig.8). It seems likely that the mound of 2-Ωm material represents a hydrothermal convection cell, driven by heat supplied from the magma reservoir beneath Kilauea summit.

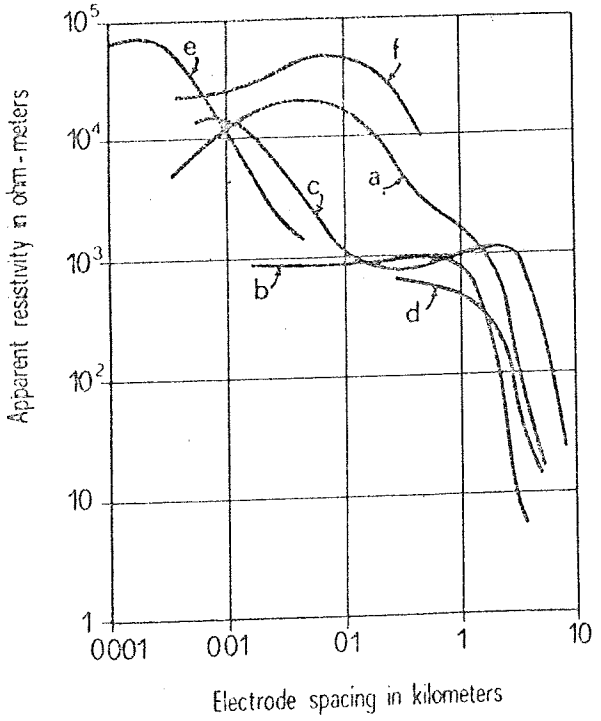

Fig.18. Seven direct-current resistivity soundings made on the island of Hawaii. Soundings *c* and *e* were made in the vicinity of Kilauea summit.

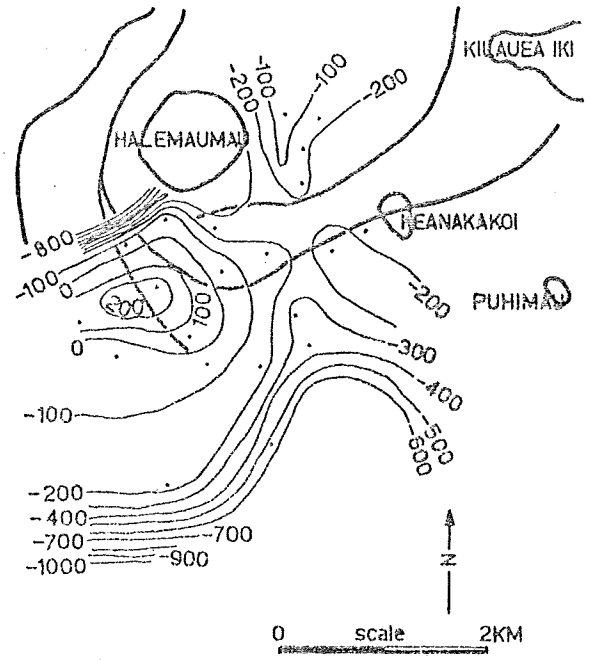

Fig. 19. Contour map of the top of a low-resistivity 2 Ωm layer beneath the summit area of Kilauea Volcano. The contours in metres are relative to sea level. The average elevation of the area is 1,100 m.

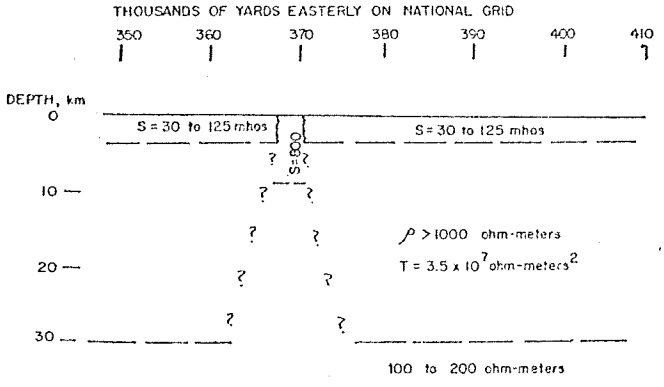

Fig. 20. Electrical cross-section along a profile crossing the thermal area of North Island, New Zealand, in the vicinity of Broadlands. S is the product of conductivity and thickness in the surface layer, and T is the product of resistivity and thickness in the second layer.

The above results were confirmed by a subsequent time-domain electromagnetic sounding survey and a DC mapping survey carried out on Kilauea Volcano during the summer of 1971 (Keller et al., 1974). In this survey, a larger dipole source was used, about 5 km long, in order to increase the dipole source moment, and measurements were carried out as far from the source as 15 km. The vertical and horizontal configurations of the top of the 2-Ωm mound were better defined. Moreover, a small mound with the same resistivity value was detected, at a depth relative to the surface of about 800 m, just south of the Keanakakoi crater, which erupted during August 1971. Such a fact gives a clear confirmation of the hypothesis that the existence and the configuration of the 2-Ωm layer is in connection with a geothermal system directly correlated with the magmatic masses feeding the volcanic activity of Kilauea.

Rapolla (1973) reports instrumental characteristics and interpretative procedures for a time-domain electromagnetic sounding survey carried out at Lipari, Aeolian Islands, Italy. A low-resistivity-layer, 3 Ωm, was found at a depth of about 1,000 m, which was interpreted as due to the presence of a geothermal system.

An example of very deep electromagnetic sounding is reported by Keller (1971b). An extensive survey using a time-domain wire-loop technique was carried out in the volcanic region of North Island, New Zealand. A 30-kVA motor generator set was used as a power source. Attention was given to minimizing the contact resistances which were reduced to values as low as 5—10 Ω, despite the fact that surface rocks had a resistivity of 1,000 Ωm or more. With such conditions, a step current of up to 60 A was driven into the ground.

The results of the survey are shown on an electrical cross-section in Fig.20. The electrical structure of crust and upper mantle below the investigated area was sketched. In particular, the presence of a low resistivity zone, 100—200 Ωm, in the lower crust and upper mantle, was pointed out. A result of great interest for the understanding of the origin of the local volcanic activity lies in the fact that the depth of this conductive zone decreases from 25—30 km to about 10 km just inside a narrow belt, where most of the geothermal manifestations occur.

Magneto-telluric sounding

In a magneto-telluric determination of earth resistivity, one measures the simultaneous magnitudes of orthogonal electric and magnetic field components, normally present as electrical noise (Keller, 1971c). By assuming that these components belong to a planar electromagnetic wave, propagating vertically into the Earth, the earth resistivity can be computed quite simply. In principe, the magneto-telluric method has advantages over both the dipole mapping method, in that it is an inductive

method, and the electromagnetic method, in that no strong source of an electromagnetic field needs to be provided. The disadvantages of the method are that measurements must be made at a single site for a moderately long period to obtain the required data, and that extensive data processing is required to convert the measured values into a resistivity sounding curve. Magneto-telluric soundings may be carried out using either low frequencies, from 0.001 to 10 Hz, or high frequencies, from 20 Hz to 20 kHz. No low-frequency magneto-telluric surveys in thermal areas have been reported, but some applications of high-frequency magneto-telluric surveys to geothermal exploration have been made (Keller, 1971b). The essential elements of an audio-frequency magneto-telluric field system (AMT) and the formula for computing resistivity are shown in Fig.21.

In the AMT method, measurements are made at a sequence of discrete frequencies, ranging from 20 Hz to 20 kHz. At a specific frequency, the resistivity so determined is an average for rocks to a depth of one skin-depth. The skin-depth of an electromagnetic wave is determined from the frequency and the resistivity of the rock through which it is passing. Skin-depth may be determined from a chart, such as the one shown in Fig.22.

When magneto-telluric measurements are made at audio-frequencies, the source of energy is usually either currents flowing in power mains or energy arriving from distant lightning strokes. The wave-lengths range

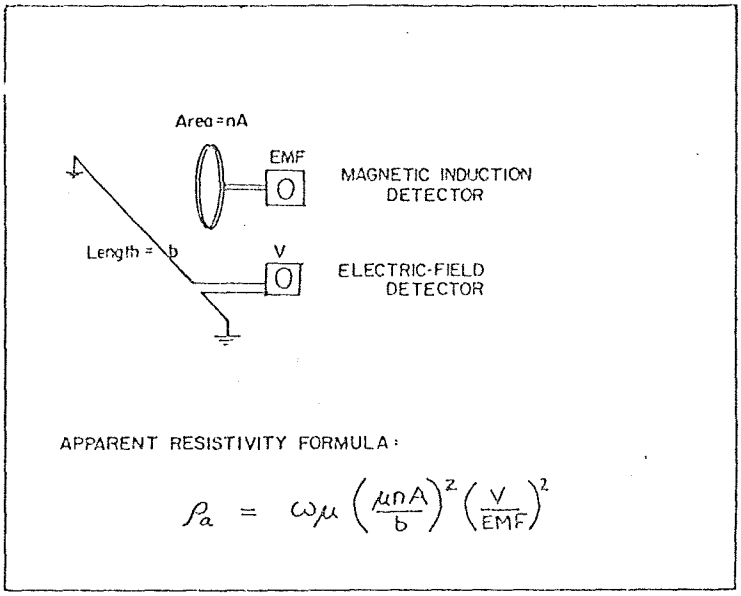

Fig.21. Audio-magneto-telluric surveying system. ω = pulsation; μ = magnetic permeability; V = voltage; EMF = electromotive force.

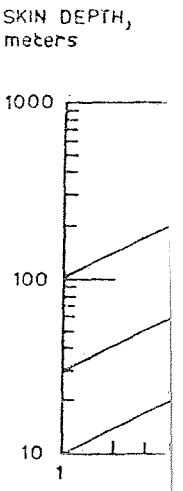

Fig.22. Skin-de

from a few t
the Earth.

Instrumen
copper elect
between the
selected arbi
component o
is detected
sensitivity mi
ceramic core
trode line a
voltmeters h
repeated with
range of inte
Lake Managu
in Fig.23. Th
and in its
Momotombo
summit lying
eruption of
Lake Managu

The AMT
In a pseudo-s
depth; other

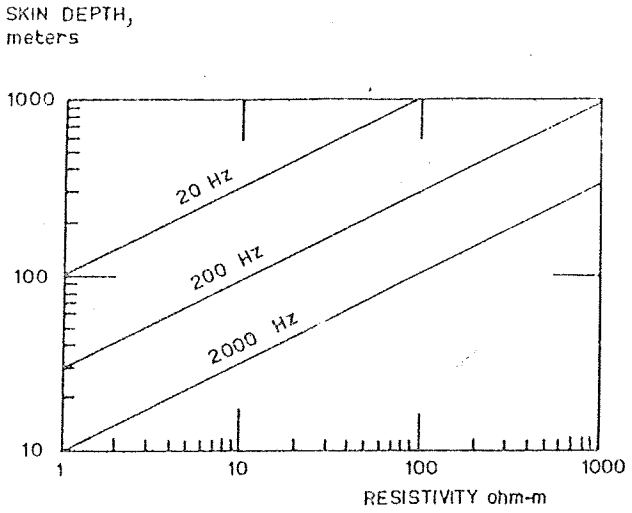

Fig.22. Skin-depth chart.

from a few tens of metres to some hundreds of metres, when measured in the Earth.

Instrumentation is simple. Electric fields can be determined by using copper electrodes driven about 15 cm into the soil, with a separation between them of the order of 20 m. The separation of the electrodes is selected arbitrarily, to provide a measurable signal level. The horizontal component of magnetic induction, at right angles with the electrode line, is detected with an induction coil. An induction coil with adequate sensitivity might consist of 10,000 turns of wire wound on a permeable ceramic core, with an area of 0.01 m^2. The voltages from both the electrode line and the induction coil are measured with sensitively-tuned voltmeters having a sensitivity of 0.1 μV or better. Measurements are repeated with the voltmeters tuned at a sequence of frequencies over the range of interest. An example of AMT survey made along the shore of Lake Managua, on the flank of Momotombo Volcano, Nicaragua, is shown in Fig.23. The thermal manifestations along the shore of Lake Managua, and in its vicinity, are the most extensive in western Nicaragua. Momotombo Volcano rises some 1,280 m above these springs, with the summit lying about 2 km north of the area of fumarolic activity. The last eruption of Momotombo was in 1905; there are no recent flows on the Lake Managua side of the volcano.

The AMT data are presented in Fig.23, in the form of a pseudo-section. In a pseudo-section, frequency is plotted as the vertical scale, rather than depth; otherwise, the section is similar to a normal section plot. The

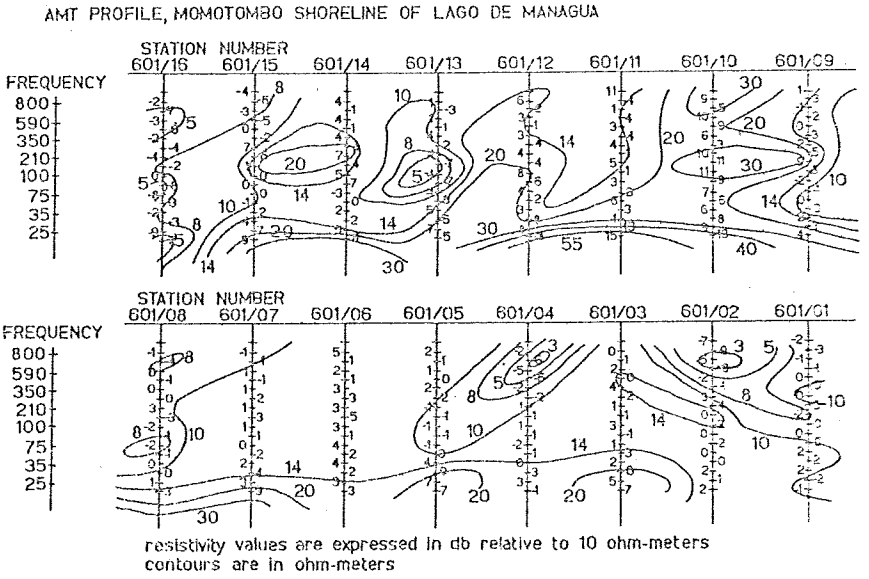

Fig.23. AMT profile, Momotombo shoreline of Lake Managua.

relationship between frequency and depth has been given previously, on the skin-depth chart, in Fig.22.

Schlumberger soundings with a minimum spacing of 1/2 km were also made along this profile, and provide some verification for the resistivities measured with the AMT method. The areas of low resistivity — 3 to 5 Ωm — near station 601/13 and 601/04-02 are also observed with the Schlumberger soundings and coincide with the location of boiling springs along the shore of Lake Managua. The area of moderately high resistivity — 30 Ωm — about station 601/10 coincides with an area over which a basalt flow crops out at the surface

APPLICATION OF ELECTRICAL SURVEYING TECHNIQUES TO GEOTHERMAL EXPLORATION

The examples of field surveys given in the preceding section should indicate that geothermal systems can be well mapped with electrical surveys.

We should now consider the proper design of an exploration programme using these techniques. The simplest technique is the audio-magneto-telluric method, and so one may assume that its proper role in an exploration programme would be in reconnaissance. At audio-frequencies, the depth to which resistivity can be determined is limited to a few

hundred metres, so the reconnaissance programme should take this into account. The use of lower frequencies to obtain deeper penetration will require an inordinate amount of work...

Following shallow reconnaissance with the AMT method, deep reconnaissance using the dipole mapping method should be considered, if surface conditions permit the use of a method with electrode contacts. With dipole-mapping, an area of about 200—300 km^2 can be mapped with a single source location.

Considering that a geothermal system with enough volume to support a power plant must have a surface area of several square kilometres, a station density of one per square kilometre should be adequate. With such a station density, a survey about a single source dipole should take no more than one week. The resistivity contours obtained with the dipole-mapping method depend, to some extent, on the geometric inter-relation between the source dipole and the conductive bodies being mapped. Because of this, successive dipoles should be sited to provide overlap of areas being surveyed, so that each receiver location can be energized from two source locations. Dipole mapping surveys provide very little information about the vertical profile of a thermal system. In planning drilling operations, it is important to know the depths to the top and bottom of the convecting system, as well as the lateral boundaries. Electromagnetic soundings and Schlumberger soundings may be used for this purpose. Because it is difficult to obtain Schlumberger soundings with spacings of more than ½—1 km in areas with pronounced lateral variations in resistivity, the use of Schlumberger soundings is limited to the determination of the depth to the top of a geothermal system. Electromagnetic sounding methods may be used to determine the depth to basement, which is normally assumed to be the base of the convecting system.

The most direct application of resistivity data to exploration for geothermal systems is in delineating the boundaries of conductive areas associated with the occurrence of hot water underground. However, resistivity data may also be used to infer more quantitative characteristics of thermal areas, under favourable circumstances. Using Fig.8, for example, the temperature of the water in a geothermal system might be estimated by noting the contrast in resistivity between rocks within the thermal zone and similar rocks outside it. An example of such a determination is illustrated by the histogram in Fig.24, a compilation of apparent resistivities measured from two dipole sources during a survey of the Dieng Plateau of central Java (Keller et al., 1974). Numerous hot springs and fumaroles occur in this area, with extensive areas of low resistivity about these surface manifestations of hydrothermal activity. Resistivity values for a single rock type commonly show a log-normal distribution, statistically (Keller, 1968). The distribution in Fig.24 appears to be the sum of several such log-normal distributions, with median values of 1.3, 6

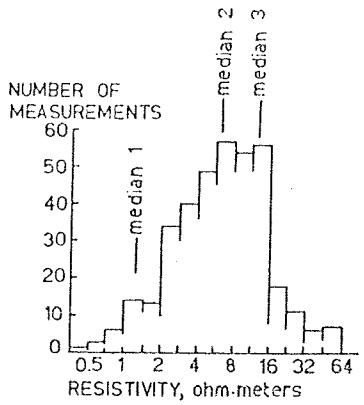

Fig.24. Histogram of apparent resistivity values determined in dipole mapping surveys. The resistivity scale is log normal.

and 12 Ωm, as indicated by the notation, medians 1, 2 and 3 on Fig.24. It may be reasonable to conclude that the median value of 1.3 Ωm applies to the hot-water saturated rock in the centres of thermal activity, the median value of 6 Ωm applies to the moderately altered and heated rock in the belt containing these centres of thermal activity, and the median value of 12 Ωm applies to "normal" volcanic rocks outside the area appreciably affected by the thermal activity.

Sampling of springs in the area (Truesdell, 1970) indicates that the pore-water resistivity should be in the range of 1.5—2.0 Ωm. Using the median of 12 Ωm as characterizing normal rocks, a formation factor of 6 to 8 is obtained.

From Fig.5, this formation factor corresponds to a porosity of about 35%. If the reduction of the resistivity in the belt containing the thermal centres to 6 Ωm is caused only by increased temperature, the curves in Fig.8 indicate that a temperature rise from 20°C to 55°C would be required. The decrease in resistivity of the rock in the centres of thermal activity by a factor of 7—9 indicates that the temperature of the convecting systems may be as high as 250°C. However, it must be considered that the convecting hot-water systems may cause locally increased porosity, and may be somewhat more saline than waters in normal rocks. These two factors may decrease the resistivity in the same manner as increased temperature does.

The electrical survey data can be used, in many cases, to arrive at a highly speculative estimate of the power-producing potential of a geothermal area. The volume of a geothermal system can be estimated from the areal extent of the anomaly in resistivity it causes and the depth to basement. According to Banwell (1970), the heat energy available on

cooling hydrothermal fluids from 250°C to 50°C is 3,500 MW-years per km^3 of reservoir. Nowhere near all this energy is available in the form of electrical energy, because of inefficiencies in production and conversion; Banwell gives a realizable yield as being 900 MW-years per km^3 of the reservoir. Thus, if the volume of the reservoir is estimated from an electrical resistivity survey, the capacity of a generating plant that can be supported is the product of the volume by Banwell's estimate of the convertible energy, divided by the number of years over which the reservoir is to be produced to exhaustion.

MAGNETIC AND ELECTRICAL ANOMALIES CORRELATED WITH VOLCANIC ERUPTIONS

One of the main themes in physical volcanology is at the present time the prediction of eruptions. Statistical analyses of seismic activity (Minakami, 1973) and measurements of ground deformation (Kinoshita et al., 1974) seem, up to now, to give the most reliable tool for such a prediction. However, the great importance of the problem, and the failure of both methods on some occasions, demand the development of other methods, based on different geophysical parameters.

Keller et al. (1972c) report observation of unusual magnetic noise preceding the Kilauea, August 1971, summit eruption (Fig.25,26). Such a noise was detected during an electromagnetic survey of the volcano by recording the voltage output from a coil of wire lying on the ground. Noise was detected 23 days before the eruption near the Keanakakoi crater, about 150 m away from a fissure which became active during the eruption. As an explanation for this anomaly, the above-mentioned authors put forward the hypothesis that the magma intruded near the surface to form a conductive zone, in which induction from magnetic micropulsations would take place. Magnetic micropulsations are characterized by fluctuations in the Earth's magnetic fields with an amplitude of one gamma or less, and with periods of ten seconds, or larger. The induced current flow in the Earth is proportional to the Earth conductivity. The secondary magnetic field, resulting from the induced currents, is normally directed in the horizontal plane. However, when there are strong lateral changes in conductivity, the secondary magnetic field may have a significant vertical component, which could be detected by a horizontal coil.

Johnston and Stacey (1969) observed magnetic anomalies associated with the April 1968 eruptions of Mount Ruapehu Volcano, New Zealand. They recorded the difference in the total magnetic field on an 8-km baseline. Anomalies of tens of gammas were recorded hours before the eruptions. The physical process that the authors think is more consistent for explaining these magnetic anomalies is the piezomagnetic effect. The

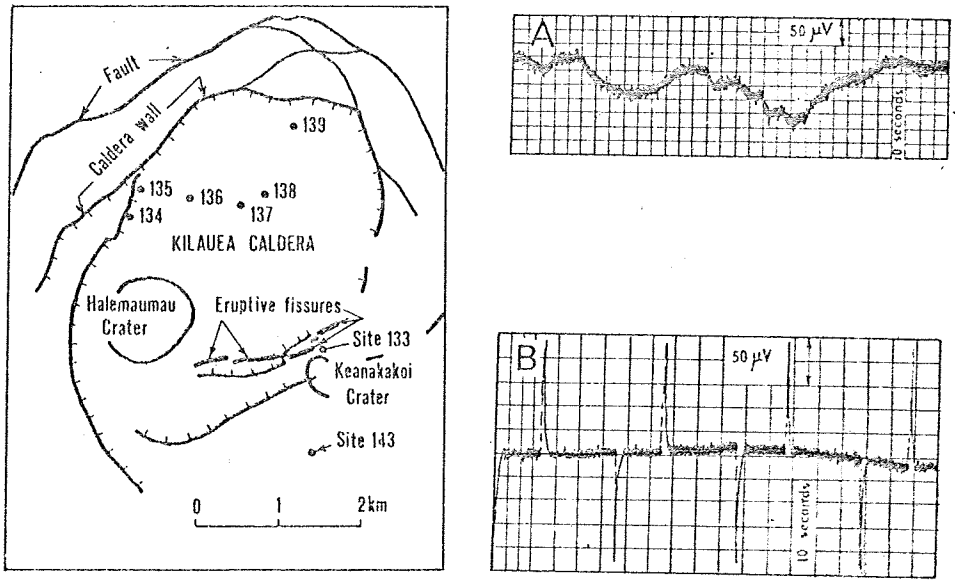

Fig. 25. Map of the summit of Kilauea Volcano showing the location of the eruption of August 14, 1971 and the sites where electromagnetic field records were made. Other recording sites lie off the map. Site 133 was the only location where the unusual magnetic noise was recorded. Caldera faults are as indicated by Petersen (1967) in the U.S.G.S. map GD-667. (From Keller et al., 1972c.)

Fig. 26. Sections of records of the voltage produced from a vertical-axis induction loop with an effective area of 151,000 m^2. A. At recording site 133, on the edge of Keanakakoi Crater. The record was obtained at approximately 15h30 local time, 22 July 1971, and exhibits an unusually high noise level. B. At recording site 115, on 16 July 1971. This record shows typical background noise levels. The spikes with alternating polarity are the transient electromagnetic signals transmitted from the grounded-wire source and are not related to the phenomenon being discussed here. (From Keller et al., 1972b.)

above-mentioned authors calculate that the observed magnetic changes require a pre-eruption stress increase not less than 75 kg/cm^2.

Long-term magnetic anomalies associated with volcanic activity were reported by Rikitake and Yokoyama (1955) for some Japanese volcanoes. Magnetization and thermal demagnetization of volcanic rocks near the Curie point were considered to be the causes of the above anomalies. An alternative interpretation, relating such magnetic variations to gradual heating, from beneath, of the masses below the volcano, was put forward by Uyeda (1961).

The above examples refer only to magnetic anomalies. Electrical field anomalies, which are associated with magnetic ones, should also be detectable.

Long-term anomalies seem to be related to heating effects and should

be then related to continuous activity periods. Medium-term and short-term anomalies, which are of the most interest for prediction of eruptions, seem to be related to the fact that the presence of a molten magmatic mass at moderate depth during the pre-eruptive stage constitutes by itself an anomaly in the electrical and magnetic properties of the shallow volcano-forming masses. Finally, very short-term anomalies should be those related to the movement of magmatic masses along fissures or vents just before the eruption, either because of the stress increase they produce, or because they may behave as a conductor material moving in the Earth's magnetic field.

Proper continuous recording of magnetic and electrical fields in active volcanic areas will probably lead to a better knowledge of such anomalies and to a better comprehension of the physical phenomena involved.

In conclusion, from the above examples and others reported in the literature, it seems that magnetic and associated electrical anomalies correlated with volcanic eruptions may become, in the near future, another valuable tool for the prediction of eruptions.

REFERENCES

Banwell, C.J., 1970. Geophysical techniques in geothermal explorations. *U.N. Symp. Development and Utilization of Geothermal Resources, Pisa, Sect.* 4: 1—50.

Carrara, E. and Rapolla, A., 1972. Shallow DC resistivity surveys of the Phlegraean Fields volcanic area, Naples, Italy. *Boll. Geofis. Teor. Appl.*, 14(53/54): 34—40.

Eisenberg, D. and Kaufmann, W., 1969. *The Structure and Properties of Water.* Oxford Univ. Press, Oxford, 296 pp.

Frischknecht, F.C., 1967. Fields about an oscillating dipole. *Q. Colo. School Mines*, 62(1): 326 pp.

Furgerson, R.B., 1970. *A Controlled-Source Telluric Current Technique and its Application to Structural Investigations.* Thesis, Colorado School of Mines, Golden, Colo., T-1313: 123 pp.

Harthill, N., 1969. *Deep Electromagnetic Sounding, Geological Considerations.* Thesis, Colorado School of Mines, Golden, Colo., T-1257: 131 pp.

Imbo', G., 1968. Sulla viscosità magmatica. *Riv. Stromboli*, N. Ser., 10: 1—15.

Jackson, D.B. and Keller, G.V., 1972. An electromagnetic sounding survey of the summit of Kilauea Volcano, Hawaii. *J. Geophys. Res.*, 77(26): 4957—4965.

Jacobson, J.J., 1969. *Deep Electromagnetic Sounding Technique.* Thesis, Colorado School of Mines, Golden, Colo., T-1252: 136 pp.

Johnston, M.J.S. and Stacey, F.D., 1969. Transient magnetic anomalies accompanying volcanic eruptions in New Zealand. *Nature*, 224(5226): 1289—1290.

Keller, G.V., 1960. Physical properties of tuffs of the Oak Springs formation, Nevada. *U.S. Geol. Surv. Prof. Pap.*, 400 B: B396—B400.

Keller, G.V., 1961. Electrical properties of a part of the Portage Lake lava series, Houghton County, Michigan. *U.S. Geol. Surv. Prof. Pap.*, 424-D: D272—D274.

Keller, G.V., 1962. Electrical resistivity of rocks in the area 12 tunnels, Nevada test site, Nye County, Nevada. *Geophysics*, 27(2): 242—252.

Keller, G.V., 1968. Electrical prospecting for oil. *Q. Colo. School Mines*, 63(2): 268 pp.

Keller, G.V., 1971a. Electrical characteristics of the Earth's crust. In: J.R. Wait (Editor), *Electromagnetic Probing in Geophysics*. Golem Press, Boulder, Colo., pp. 13—76.

Keller, G.V., 1971b. Induction methods in prospecting for hot water. *Geothermics (1970), Spec. Iss.*, 2: 318—332.

Keller, G.V., 1971c. Natural-field and controlled-source methods in electromagnetic exploration. *Geoexploration*, 9(2/3): 99—148.

Keller, G.V. and Frischknecht, F.C., 1966. *Electrical Methods in Geophysical Prospecting*. Pergamon, Oxford, 517 pp.

Keller, G.V., Pritchard, J.I. and Anderson, L.A., 1972a. Geoelectric studies on the island of Hawaii. *U.S. Geol. Surv. Prof. Pap.* (in press).

Keller, G.V., Jackson, D.B. and Rapolla, A., 1972b. Observation of unusual magnetic noise preceding the August 1971 summit eruption of Kilauea Volcano. *Science*, 175: 1457—1458.

Keller, G.V., Jackson, D.B. and Rapolla, A., 1974. A comparison of several electrical prospecting techniques at Kilauea Volcano, Hawaii. *Geophysics* (in press).

King, C.A., 1971. *Time-Domain Electromagnetic Coupling*. Thesis, Colorado School of Mines, Golden, Colo., T-1427: 60 pp.

Kinoshita, W.T., Swanson, D.A. and Jackson, D.B., 1972. The measurement of crustal deformation related to volcanic activity at Kilauea Volcano, Hawaii. In: P. Gasparini, L. Civetta, A. Rapolla and G. Luongo (Editors), *Physical Volcanology*. Elsevier, Amsterdam, pp. 87—115.

Koyanagi, R.Y. and Endo, E.T., 1971. Hawaiian seismic events during 1969. *U.S. Geol. Surv. Prof. Pap.*, 750C: C158—C164.

Minakami, T., 1972. Prediction of volcanic eruptions. In: P. Gasparini, L. Civetta, A. Rapolla and G. Luongo (Editors), *Physical Volcanology*. Elsevier, Amsterdam, pp. 313—333.

Parkhomenko, E.I., 1967. *Electrical Properties of Rocks*. Plenum, New York, N.Y., 314 pp.

Quist, A.S. and Marshall, W.L., 1966. Electrical conductances of aqueous solutions at high temperatures and pressures III. The conductances of potassium bisulfate solutions from 0 to 700° and at pressure to 4000 bars. *J. Phys. Chem.*, 72: 3714.

Quist, A.S. and Marshall, W.L., 1968. Electrical conductances of aqueous sodium chloride solutions from 0 to 800° at pressures to 4000 bars. *J. Phys. Chem.*, 72: 684.

Rapolla, A., 1973. Strumentazione ed esempio di applicazione dei sondaggi elettromagnetici profondi in un area vulcanica attiva (Lipari, Isole Eolie). *Riv. It. Geofis.*, 22: 111—116.

Rikitake, T. and Yokoyama, I., 1955. Volcanic activity and changes in geomagnetism. *J. Geophys. Res.*, 60: 165.

Silva, L.R., 1969. *Two-Layer Master Curves for Electromagnetic Sounding*. Thesis, Colorado School of Mines, Golden, Colo., T-1250: 80 pp.

Truesdell, A.H., 1970. Preliminary geochemical evaluation of the Dieng Mountains, Central Java, for the production of geothermal energy. *U.S. Geol. Surv. Open File Rep.*.

Uyeda, S., 1961. An interpretation of the transient geomagnetic variations accompanying the volcanic activity at Volcano Mihara, Oshima Island, Japan. *Bull. Earthq. Res. Inst.*, 39: 579—591.

Watanabe, H., 1970. Measurements of electrical conductivity of basalts at temperatures up to 1500°C and pressure to about 20 kilobars. *Spec. Contrib., Geophys. Inst. Kyoto Univ.*, 10: 159—170.